Electromagnetic characterization of planar metamaterials by oblique angle spectroscopic measurements

T. Driscoll and D. N. Basov
Physics Department, University of California-San Diego, La Jolla, California 92093, USA

W. J. Padilla
Department of Physics, Boston College, Chestnut Hill, Massachusetts 02467, USA

J. J. Mock and D. R. Smith
Electrical and Computer Engineering Department, Duke University, Durham, North Carolina 27708, USA
(Received 18 June 2006; revised manuscript received 11 December 2006; published 13 March 2007)

Artificially structured metamaterials with unit-cell dimensions on the order of 1/10th of a wavelength ($\lambda/10$) have been shown to be well approximated by an effective medium description which mimics a continuous material. In this paper we present data for transmission and reflection from a planar array of split-ring resonators (SRRs) at varying angles of incidence. We attempt to model the form of the angle—dependent response of the SRRs using the Fresnel equations formulated from effective medium theory—treating the array as a thin continuous anisotropic crystal. This model is then fit to experimental data taken on a planar array of split rings to gauge the model accuracy, and to produce values for the frequency-dependent permeability and permittivity of the experimental SRR array. Simultaneous fitting of the transmission and reflection at multiple angles helps to avoid multiple solutions for the permittivity and permeability. This forward fitting approach using multiple angles is advantageous, as it enables a characterization of the optical constants without the need for phase information, and it avoids many of the branch problems inherent in the numerical inversion methods used so far on metamaterials. The work presented here shows the feasibility of this method. A refined procedure will be particularly advantageous for experimental characterization of higher frequency structures (i.e., THz and above), where phase information is difficult or impossible to obtain.

DOI: 10.1103/PhysRevB.75.115114 PACS number(s): 78.20.Ci, 78.20.Bh, 41.20.Jb

BACKGROUND

In the absence of magnetoelectric coupling, the electromagnetic response of a continuous medium can be entirely described in terms of its three-by-three electric permittivity $\underline{\underline{\varepsilon}}(\omega)$ and magnetic permeability $\underline{\underline{\mu}}(\omega)$ tensors which together represent the crystal's response to light at any frequency along any direction in three dimensions. These tensors are macroscopic bulk parameters that encapsulate the microscopic motion of responding dipoles and currents.[1] Once these material property tensors are determined, the Fresnel equations can be derived from Maxwell's equations[2] by solving the appropriate electromagnetic boundary-value problem at the various material interfaces. The Fresnel equations describe the reflection and transmission of polarized light incident at any angle to a planar layer or stack of layers of one or more materials.

Metamaterials have recently garnered much attention because of their ability to achieve unusual electromagnetic responses, such as negative index, not typically found in natural materials.[3,4] Loosely defined, a metamaterial is an artificial crystal in which mesoscopic inclusion structures replace the microscopic atoms or molecular structures of natural materials. So long as the scale of the periodicity of the metamaterial is significantly smaller than the wavelengths of interest, the metamaterial is electromagnetically indistinguishable from a continuous material. Most reported metamaterials have a periodicity ($\mathbf{P}$) that is usually on the order of $\mathbf{P}\sim\lambda/10$, which contrasts with natural crystals for which the Wigner-Seitz unit-cell may be 5 A, corresponding to $\mathbf{P}\sim\lambda/1\times10^{8}$ at microwave frequencies. Nevertheless, it has been shown that macroscopic approximations such as the permittivity and permeability tensors remain largely valid for these metamaterials,[5] and the permittivity and permeability description has shown considerable success in describing the behavior of electromagnetic scattering from metamaterial samples.

If metamaterials are to be treated on the same basis as natural materials, it is necessary to define a procedure by which the permittivity and permeability tensors can be determined for a metamaterial. To date, two rigorous methods have been introduced to retrieve the material parameters from simulated or measured metamaterial structures: the field averaging method and the *S*-parameter retrieval method. In the field averaging method, which can be readily applied to simulated metamaterial structures, the local electric and magnetic fields are averaged over surfaces and edges to arrive at macroscopic values for the $\mathbf{E}$, $\mathbf{D}$, $\mathbf{B}$, and $\mathbf{H}$ fields. From these macroscopic averaged field values, the tensor elements for the permittivity and permeability tensors can be found. In the *S*-parameter retrieval method, the scattering parameters (or reflection and transmission amplitudes and phases) for a finite length of metamaterial are either computed or measured.

The *S*-parameters retrieval method has now been widely applied for the characterization of metamaterial structures at rf and microwave frequencies.[6,26] *S*-parameters contain both amplitude and phase information, and so a single frequency

S-parameters measurement yields four values that can in turn be inverted to find the real and imaginary permittivity and permeability components transverse to the given direction of propagation. While the method does not provide unique solutions due to the nature of the required numerical inversion, typically erroneous solutions can be excluded by studying the retrieved parameters over a large enough frequency band that unphysical branch jumps can be identified.

The *S*-parameters retrieval method suffers from several drawbacks: The difficulty in obtaining phase information at THz and higher frequencies renders the *S*-parameter retrieval method impractical. Therefore, characterization of metamaterial samples at infrared frequencies has relied on the consistency of transmission and reflection magnitudes with simulation results. This approach has enabled the assignment of magnetic or electric responses to fabricated metamaterials, but has not resulted in a direct quantification of material properties for THz and higher frequency structures.[7,8] In addition, most work to date has been restricted to wave incidents along one of the three primary axes, since this orthogonal geometry is far more convenient for both numerical simulation and analytical expressions.

However, since the Fresnel equations can be generated for oblique incidence waves, measurement of the reflected or transmitted wave magnitude for multiple angles provides additional information that can be used to compensate for the absence of phase data. In particular, the reflection and transmission coefficients corresponding to waves at varying incident angles contain different relative contributions of the material parameter tensor elements; and thus by collecting transmission or reflection data at a number of angles, it is possible to arrive at an over-determined system of equations for $\underline{\underline{\varepsilon}}(\omega)$ and $\underline{\underline{\mu}}(\omega)$ that can be solved by known methods. The Fresnel formulation thus provides a rigorous method for determining $\underline{\underline{\varepsilon}}(\omega)$ and $\underline{\underline{\mu}}(\omega)$ of a structure from experimental data in any material where $\underline{\underline{\varepsilon}}(\omega)$ and $\underline{\underline{\mu}}(\omega)$ can be safely defined. While it should be possible to perform this characterization at every given frequency, a great computational simplification occurs if the material is modeled as a collection of electric and magnetic oscillators whose functional forms are known. By fitting the parameters for these oscillators to the measured data, fewer experimental frequency points need be acquired and calculation complexity for fitting is considerably reduced. This approach is common and well documented in the field of optical spectroscopy. The software package WVASE,[9] for example, is a common tool to do this analysis in a non-magnetic $[\underline{\underline{\mu}}(\omega)=1]$ crystal.[10]

In this paper, we attempt to use the Fresnel approach to describe the transmission and reflection through a metamaterial at a variety of angles. The frequency-dependent functional form for the double- split-ring resonator (SRR) structure has been previously investigated and reported upon,[11] so we apply a spectroscopic approach here, modeling the metamaterial as a collection of magnetic and electric oscillators. The success of the Fresnel method applied to a metamaterial relies upon the entirety of the metamaterial electromagnetic scattering response being governed by a well-defined permittivity and permeability. This has been shown to be largely true, although new revisions to effective medium theory continue to account for artifacts such as periodicity and diffraction.[12,13]

One last point to be made is that for infrared and higher frequencies, metamaterial test samples usually comprise a single plane of lithographically patterned conducting elements, with thickness much less than the wavelengths of interest, i.e. $\sim\lambda/300$. The scattering problem, then, should properly be formulated as a boundary value problem for which electric and magnetic polarizabilities can be defined for the intervening metamaterial layer. Here, we introduce an effective thickness d for the metamaterial layer that will facilitate the assignment of effective bulk permittivity and permeability. Physically, this effective thickness may be thought of as a representation of the distance that the local fields extend out away from the metamaterial plane. If d is on the order of the unit cell dimension in the plane, then the resulting effective medium parameters generally predict the scattering behavior of a composite medium formed by stacking multiple planar samples together spaced d apart. However this holds true only asymptotically—if the expected composite sample consists of planes stacked with an intervening distance that is less than **P**, then cell-to-cell interactions between planes invalidate the use of a single layer to predict the response of the crystal.[14] While this ambiguity is of concern, we note that it is inherent to other retrieval techniques (e.g., *S*-parameters retrieval) for which the effective medium parameters are also often derived from a single layer of metamaterial unit cells. The *s*-parameter method, even when also relying on the effective thickness of a single layer, has still proved to be quite accurate.[3,26]

To show support for the use of an effective thickness parameter in our case, we analyze numerical results for the resonant field distribution in our structure, and show interlayer interactions can be safely neglected for our structure. Fig. 1 plots the in-plane electric and out-of-plane magnetic fields extending away from our SRR structure for two cases: in a single layer planar array, and in an infinite crystal. We notice that in both cases, the induced fields have almost entirely died out by the edge of the unit cell. Also of importance is that the field distributions for the single layer and infinite crystal are quite similar. The smaller overall amplitudes of the fields for the single layer are a result of energy loss at the PML cell boundary—not present in the stacked layer. These results suggest that a single layer taken to have effective thickness d will closely approximate the permittivity and permeability of many layers placed with spacing d. An experimental probe of the unit-cell fields and effective thickness is planned for the near future to further investigate this.

EXPERIMENT

We fabricated a planar array of SRR's designed to have distinguishable electric and magnetic resonances. This copper-on-FR4 (Ref. 15) array was etched using lithography techniques typical to printed circuit boards, which have been described elsewhere. We opt for the Dual-SRR configuration shown in Fig. 2, which has been used in previous experiments.[16–18] This planar sample is placed in a micro-

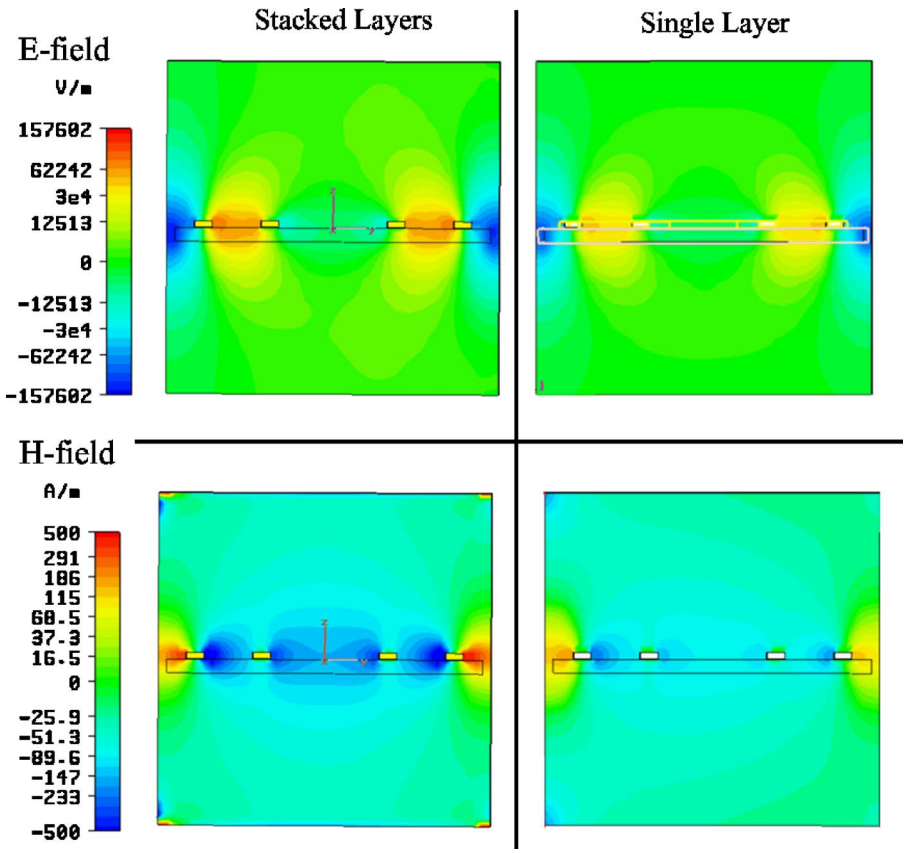

FIG. 1. (Color online) Numerical FDTD results for a cross section of the electric and magnetic distributions in our SRR structure for both a single layer and infinitely stacked layers. The fields plotted are **E** in the sample plane, and **B** normal to the sample plane. The center insert shows the geometry of the 2D field slice relative to the SRR.

wave transmission or reflection setup using polarized horn-lens assemblies driven and analyzed by a vector-network-analyzer. Transmission and reflection amplitude data was collected for *s*-polarized microwaves from 0° (normal) to 50° in transmission and from 25° to 50° in reflection. Figure 3 illustrates this setup. The reflection data is limited in angle to a minimum of 25° due to the physical size of the horns. Data is collected in frequency over the horn or lens useable range of 10 GHz to 20 GHz.

Figure 4(a) shows the collected transmission data for angles 0°, 20°, and 40° (symbols). Figure 4(b) shows the reflection data for angles 25° and 40° (symbols). In both spectra sets, we can identify one predominate feature: a narrow angle-dependent response near 14 GHz. There is also a broad trend in each data: decreasing transmission (increasing reflection) with frequency. As discussed in previous literature,[19] an individual SRR element exhibits in-plane electric and out-of-plane magnetic responses—as well as magnetoelectric coupling. The magnetoelectric coupling can be eliminated in a bi-isotropic array such as ours, with reflection symmetry about the mirror lines ζ and Γ (see Fig. 2).[20] The magnetic response of the SRR involves magnetic flux passing through its nearly-closed loops. This flux is zero for normal incidence (θ=0°) light and increases as the incidence becomes more oblique. The electric response of a SRR comes from the sides acting as cut-wire dipole antennae.

Returning to the experimental data in Fig. 4, we attribute the narrow feature at 14 GHz to the magnetic response of the SRR. The feature is absent in the transmission data at 0° where the applied magnetic field is in-plane, and grows as the incident angle becomes more obtuse and we include normal components of **B** which interact with the SRR. The broad trend of decreasing transmission (increasing reflection) is part of the electric interaction—it is the onset of the higher frequency electric resonance.

THEORY

To attempt to describe, predict, and characterize the angle-dependant response of the SRR, we turn to an effective medium picture, and solve for the Maxwell's equations boundary value problem for transmission and reflection through our sample. The electromagnetic response of the resulting composite planar sample is then described as follows: Electric fields along the two sides of the composite induce an electric dipolar response (in the $\hat{x}$ and $\hat{y}$ directions), and magnetic fields that penetrate the SRR loops (in the $\hat{z}$ direction) induce a magnetic dipolar response. We then assign the tensors

$$\underline{\underline{\varepsilon}}(\omega) = \begin{pmatrix} \varepsilon_{xx}(\omega) & 0 & 0 \\ 0 & \varepsilon_{yy}(\omega) & 0 \\ 0 & 0 & 1 \end{pmatrix} \underline{\underline{\mu}}(\omega) = \begin{pmatrix} 1 & 0 & 0 \\ 0 & 1 & 0 \\ 0 & 0 & \mu_{zz}(\omega) \end{pmatrix}. \tag{1}$$

The response of ε_{yy} is considerably more complicated than that of ε_{xx} due to the asymmetry of SRR sides lying in the $\hat{y}$ direction, so we confine **E** to the $\hat{x}$ direction (*s* polarization) using linearly-polarized incident light, as indicated by Fig. 3.

Working from these tensors, we now summarize the Fresnel equations for the reflection and transmission of light

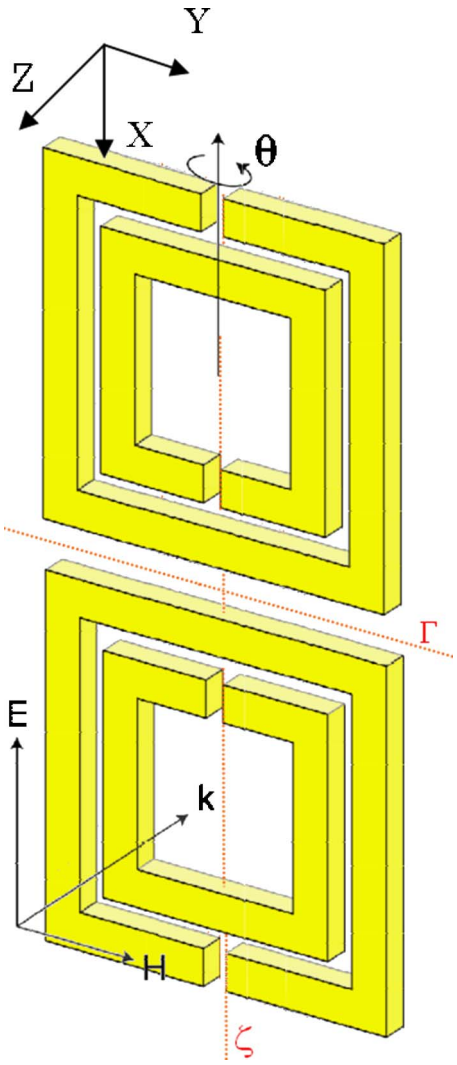

FIG. 2. (Color online) SRR dimensions in mm: w=2, t=0.13, g=0.35, c=0.47, L=2.4. The vertical thickness of the copper is ~37 μm (1 oz. copper).

incident along vacuum wave vector **k** on a planar layer of stratified material, where k is at an incidence angle θ from the normal ($\hat{z}$ direction). Although we restrict our analysis to s-polarized light, the procedure for p-polarization follows from the duality of **E**, **H**. This is a three region boundary value problem,[21,2] with the continuity of $\mathbf{E}_x$ and $\mathbf{H}_y$. Maxwell's equations are written as

$$\nabla \times \mathbf{H} = -i\omega \underline{\underline{\varepsilon}} \varepsilon_0 \mathbf{E} \quad \nabla \times \mathbf{E} = +i\omega \underline{\underline{\mu}} \mu_0 \mathbf{H}. \tag{2}$$

Combining these to get the wave equation and assuming sinusoidal dependence of all solutions, we arrive at the dispersion relation inside the medium

$$\frac{q_y^2}{\mu_{zz}} + \frac{q_z^2}{1} = \omega^2 \varepsilon_{xx}, \tag{3}$$

where **q** is the wave vector in medium. Setting up forward- and backward-propagating waves in each region, and matching boundaries at each interface, we solve the system of 4 linear equations (2 generated from each boundary) to find

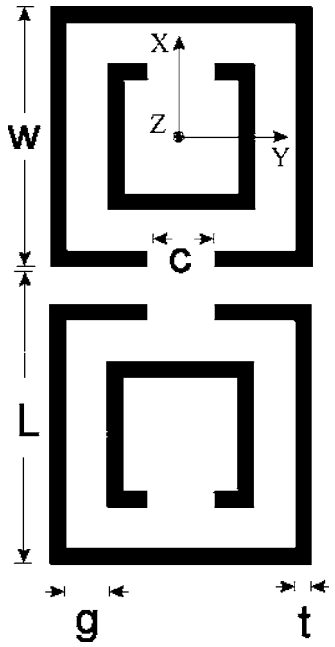

FIG. 3. The geometry of the symmetric SRR array in s polarization.

$$t = \frac{e^{-ik_z d}}{\cos(q_z d) - \frac{i}{2}\left(\frac{\mu_{zz}k_z}{q_z} + \frac{q_z}{\mu_{zz}k_z}\right)\sin(q_z d)},$$

$$r = \frac{\frac{i}{2}\left(\frac{q_z}{\mu_{zz}k_z} - \frac{\mu_{zz}k_z}{q_z}\right)\sin(q_z d)}{\cos(q_z d) - \frac{i}{2}\left(\frac{\mu_{zz}k_z}{q_z} + \frac{q_z}{\mu_{zz}k_z}\right)\sin(q_z d)}. \tag{4}$$

These are the coefficients of reflection and transmission for our system. The incident angle θ is related to the components

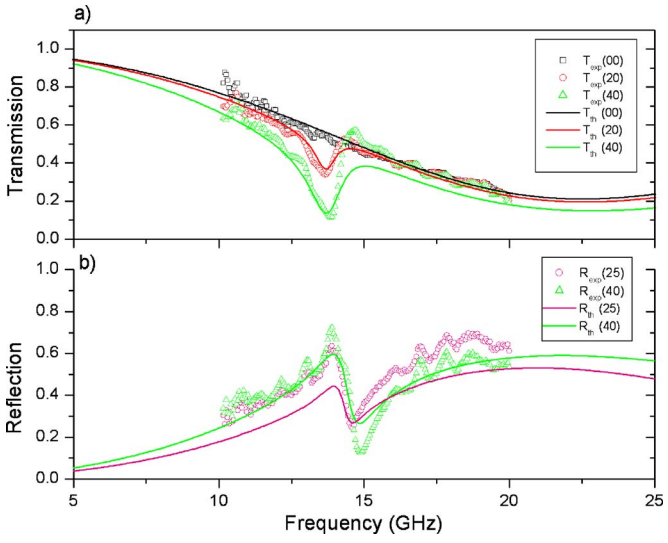

FIG. 4. (Color online) Experimental data at selected angles for transmission (0°, 20°, 40°) and reflection (25°, 40°) with a fit of the Fresnel theory. The oscillator parameters corresponding to the two fits are shown in Table I.

of the vacuum wave vector **k** and medium wave vector **q** as

$$\sin\theta = \frac{k_y}{k_0} = \frac{q_y}{k_0}. \tag{5}$$

Let us now assume some frequency dependent form for ε_{xx} and μ_{zz} to simplify the calculation, as discussed in the background section. The most accurate form for the electric and magnetic response for the symmetrized SRR configuration is [22–24]

$$\varepsilon_{xx}(\omega) = \varepsilon_s - \frac{A_e {\omega_p}^2}{\omega^2 - {\omega^2}_{e0} + i\omega\gamma_e},$$

$$\mu_{zz}(\omega) = 1 - \frac{A_m \omega^2}{\omega^2 - \omega_{m0}^2 + i\omega\gamma_m}, \tag{6}$$

where A are oscillator amplitudes, ω_p are plasma frequency, ω_0 are resonance center frequency, γ are damping-constants, and ε_s is the static (zero frequency) dielectric constant of the metamaterial. This expression for μ_{zz} has been shown to be valid over the limited frequency ranges where the composite can be considered an effective medium, despite the unphysical fact that it does not approach unity at large frequencies. Clearly, these expressions will not be valid for frequencies at which the wavelength approaches the periodicity.

ANALYSIS

We now wish to determine how well the transmission and reflection features seen in Fig. 4 are captured by this simple Fresnel model, and to evaluate the fitted values for μ_{zz} and ε_{xx}. To do this, Eq. (4) was coded into a MATLAB program that uses a combination of graphical user-feedback and least-squares minimization to choose the material parameters (A_e, A_m, ω_{m0} ω_{e0}, ω_{mP}, γ_m, γ_e, ε_s) in Eq. (6). The fitting procedure is roughly as follows: First we guess appropriate values for the center frequencies of the oscillators based on the observed data. Values for A, γ, ω_m, and ω_p are selected by hand so the fit roughly matches the features of the data. All parameters of the oscillator are then repeatedly adjusted to find the values with the smallest residue that still qualitatively matches the data. Because the forms of Eq. (6) are only a good first approximation to the actual response of our material it is necessary to do this fitting by hand to avoid a-physical solutions.

We find a relatively good qualitative agreement between the experimental data and the modeled transmission/ reflectance curves fit to the data. This fit is plotted as the solid lines in Fig. 4. The general trend of decreasing transmission (increasing reflection) with increasing frequency is captured by the higher frequency in-plane electric oscillator. The attributes of the magnetic modeled transmission dip match well to the data. The final fit parameters to transmission and reflection are given in Table I. Also given is an average residue measure of the fit: $\frac{\sum_{i=0}^{n}|y_{th(i)}-y_{\mathrm{data}(i)}|}{n}$. We notice some disagreement in the region immediately following the magnetic resonance, where experimental transmission levels 'bounce' back up—increasingly so at larger angles. The cause of this is unknown, although we suspect it is from unaccounted oscillator strengths such as may arise from extended array interactions.

TABLE I. Fit parameters from Eq. (6) for optical fit to transmission and reflection data.

Parameter	Transmission fit	Reflection fit
d	0.30 cm	0.30 cm
A_e	0.7	0.7
ω_{e0}	22.2 GHz	19.9 GHz
ω_p	62 GHz	62 GHz
γ_e	11.6 GHz	5.4 GHz
A_m	0.66	0.66
ω_m	8.0 GHz	8.3 GHz
γ_m	0.25 GHz	0.19 GHz
Avg. Residue	0.037	0.081

In reflection, we also see good qualitative matching of the features in the data. The largest discrepancies in refection are just after the magnetic dip, where levels in the model curve do not drop far enough. This corroborates the area of largest transmission discrepancy noted above, and suggests this area may be important for additional study. The disagreement at frequencies above 17 GHz is perhaps to be expected since wavelengths shrink and our effective-medium assumptions break down. As seen in Table I, the optimal fits for the transmission and reflection agree quite well for most oscillator parameters, differing significantly only in the damping factors. The reflection and transmission experiments were conducted on separately fabricated samples, so we should not demand the fitted material parameters be identical.

In both transmission and reflection fits we identify a sharp magnetic resonance with ω_{m0}=8 GHz, and a broad electric resonance around 22 GHz. These two optical parameters of interest, $\mu_{zz}(\omega)$ and $\varepsilon_{xx}(\omega)$, retrieved from our model fit, are plotted in Fig. 5. It is interesting to note that our model predicts the magnetic transmission and/or reflection response to occur at the zero crossing of the permeability. This is the magnetic plasma frequency, and the response of the metamaterial at this point is best described as a collective longitudinal mode. There is a direct analogy to the electric response of anisotropic crystals in spectroscopy, known as the Berreman mode.[25] This differs from previous work, where the magnetic response of a SRR plane was assumed—although not shown—to occur at the center frequency ω_{m0}. Certainly this feature warrants further investigation. The amplitude of the fitted permeability reaches a minimum of μ_{zz}=−9. This is somewhat larger than, but still close to, the maximally negative permeability values taken from previous retrievals on similar SRR structures.[26]

One important factor that is left out by the method presented here is the spatial dispersion associated with the finite unit cell of the metamaterial structure. This limitation is not inherent to the overall method, but is related to our assumption of ideal frequency dependent forms for the material parameters [Eqs. (6)]. We expect that, especially in the vicinity

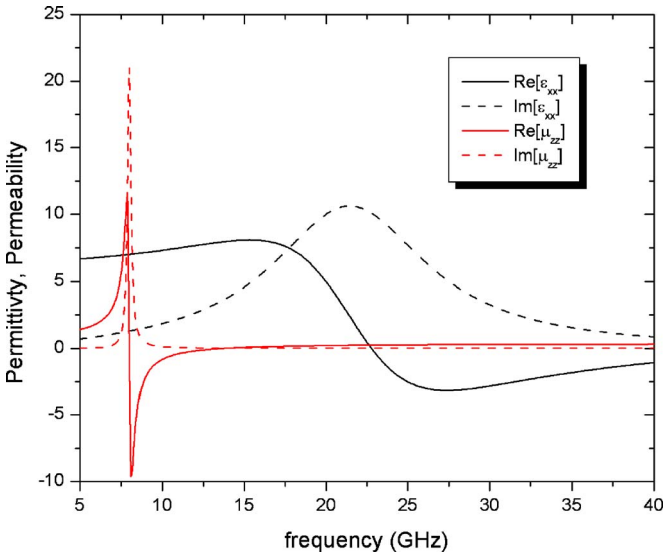

FIG. 5. (Color online) Permittivity (black) and permeability (red [gray]) dispersion curves corresponding to the transmission fit.

of the resonance, the actual values of the permittivity and permeability will be somewhat different from the values derived here. In particular, the finite size of the unit cell is known to limit the range of possible permeability values associated with the magnetic resonance,[27,5] causing significant distortions to the shape of both the real and imaginary parts of the resonance curves. For the SRR structure we have presented here, the retrieval suggests that the permeability should achieve values as large as $|\mu| \approx 9$; however, were the effects of spatial dispersion included we would expect the maximum permeability values to be significantly smaller. Work must be done to adapt this method to effective medium descriptions which include spatial dispersion.

The model fitting procedure we have outlined can be further refined by incorporating a many-oscillator routine into the algorithm, thereby enabling frequency-by-frequency fitting rather than relying on specific forms for the effective medium parameters. Such a direct retrieval will allow us to investigate the smaller features seen in the experimental data, which may not be captured by the forms in Eq. (6). In the context of a frequency-by-frequency inversion, the Fresnel equations may be used for a precise retrieval of the experimentally measured permittivity and permeability—rather than relying on the assumptions the form of Eq. (6) make. During our analysis we found that the best-fit parameter for the effective sample thickness was 3 mm, which is near enough to the unit-cell size of 2.4 mm that we expect multiple layers to behave as a good continuous medium. Future work will include investigating the accuracy of this theory on thicker, multilayer metamaterial crystals and higher frequency structures, as well as the development of a more rigorous point-by-point retrieval routine.

SUMMARY

We have shown that macroscopic permeability and permittivity tensors for a metamaterial can be used to derive Fresnel expressions for transmission and reflection from an interface at any incident angle, and that these expressions do a good job of predicting the qualitative spectroscopic features of the metamaterial. This description is quite useful, as it reduces the interaction at any angle of incidence to those fundamental magnetic and electric oscillators which the metamaterial structure mimics. Using these Fresnel expressions, experimental data for transmission (and/or reflection) at a number of angles across a broad frequency range can be used in a multiple-oscillator fitting routine to retrieve the effective-medium material parameters. The redundancy of the data at multiple angles increases the accuracy of this fitting; and it has been shown here to give reasonable values for the permittivity and permeability of a SRR two-dimensional (2D) array in the microwave range.

In the near future, we will implement a direct retrieval procedure that will avoid the use of fixed, frequency dependent forms for the material parameters. The use of such forms for metamaterials having significant spatial dispersion constrains the retrieved parameters and can yield incorrect values in the region of the resonance. Still, the method we have presented is an important step towards quantifying the electromagnetic properties of planar metamaterial samples. Having demonstrated the procedure at lower frequencies, we will shortly apply the technique to higher frequency investigations.

ACKNOWLEDGMENTS

This work was supported by DARPA through an ONR MURI and by a Multiple University Research Initiative from the Army Research Office (Contract No. DAAD19-00-1-0525).

[1] *Classical Electrodynamics*, edited by J. D. Jackson, 3rd ed. (John Wiley & Sons, New York, 1999), Chap. 1.4.
[2] *Classical Electrodynamics*, edited by J. D. Jackson, 3rd ed. (John Wiley & Sons, New York, 1999), Chap. 7.3.
[3] T. Driscoll, D. N. Basov, A. F. Starr, P. M. Rye, S. Nemat-Nasser, D. Schurig, and D. R. Smith, Appl. Phys. Lett. **88**, 081101 (2006).
[4] S. Zhang, W. Fan, N. C. Panoiu, K. J. Malloy, R. M. Osgood, and S. R. J. Brueck, Phys. Rev. Lett. **95**, 137404 (2005).
[5] Th. Koschny, P. Markos, E. N. Economou, D. R. Smith, D. C. Vier, and C. M. Soukoulis, Phys. Rev. B **71**, 245105 (2005).
[6] D. R. Smith, S. Schultz, P. Markos, and C. M. Soukoulis, Phys. Rev. B **65**, 195104 (2002).
[7] A. K. Sarychev, G. Shvets, and V. M. Shalaev, Phys. Rev. E **73**, 036609 (2006).
[8] J. Zhou, Th. Koschny, M. Kafesaki, E. N. Economou, J. B. Pendry, and C. M. Soukoulis, Phys. Rev. Lett. **95**, 223902 (2005).
[9] WVASE software by J. A. Woollam Co., Inc.

[10] H. Yao, B. Johs, and R. B. James, Phys. Rev. B **56**, 9414 (1997).
[11] M. Shamonin, E. Shamonina, V. Kalinin, and L. Solymar, Microwave Opt. Technol. Lett. **44**, 133 (2005).
[12] D. R. Smith, D. C. Vier, Th. Koschny, and C. M. Soukoulis, Phys. Rev. E **71**, 036617 (2005).
[13] Th. Koschny, P. Markos, E. N. Economou, D. R. Smith, D. C. Vier, and C. M. Soukoulis, Phys. Rev. B **71**, 245105 (2005).
[14] M. Gorkunov, M. Lapine, E. Shamonina, and K. H. Ringhofer, Eur. Phys. J. B **28**, 263 (2002).
[15] FR4 stands for Flame Retardant Laminate, a fiberglass based common circuit board material.
[16] F. J. Rachford, D. L Smith, P. F. Loschialpo, and D. W. Forester, Phys. Rev. E **66**, 036613 (2002).
[17] D. R. Smith, Willie J. Padilla, D. C. Vier, S. C. Nemat-Nasser, and S. Schultz, Phys. Rev. Lett. **84**, 4184 (2000).
[18] D. R. Smith, D. C. Vier, N. Kroll, and S. Schultz, Appl. Phys. Lett. **77**, 2246 (2000).
[19] T. J. Yen, W. J. Padilla, N. Fang, D. C. Vier, D. R. Smith, J. B. Pendry, D. N. Basov, and X. Zhang, Science **303**, 1494 (2004).
[20] D. A. Schurig, D. R. Smith, and J. J. Mock, Phys. Rev. E **74**, 036604 (2006).
[21] *Principles of Optics*, edited by Max Born and Emil Wolf (Pergamon Press, New York, 1970), Chap. 1.6.
[22] J. B. Pendry, A. J. Holden, W. J. Stewart, and I. Youngs, Phys. Rev. Lett. **76**, 4773 (1996).
[23] J. B. Pendry, A. J. Holden, D. J. Robbins, and W. J. Stewart, IEEE Trans. Microwave Theory Tech. **47**, 2075 (1999).
[24] D. R. Smith, J. J. Mock, A. F. Starr, and D. Schurig, Phys. Rev. E **71**, 036609 (2005).
[25] D. W. Berreman, Phys. Rev. **130**, 2193 (1963).
[26] A. F. Starr, P. Rye, D. R. Smith, and S. N. Nemat-Nasser, Phys. Rev. B **70**, 113102 (2004).
[27] D. R. Smith, D. C. Vier, Th. Koschny, and C. M. Soukoulis, Phys. Rev. E **71**, 036617 (2005).